HEFAT2012
9th International Conference on Heat Transfer, Fluid Mechanics and Thermodynamics
16 – 18 July 2012
Malta

LAGRANGIAN MODEL FOR DEPOSITION FROM LOW-CONCENTRATED PARTICLES-LADEN TURBULENT JETS

Terfous A., Chiban S.*, Ghenaim A., Poulet J. B. and Elahcene O.
*Author for correspondence
Laboratoire de Génie de la Conception LGeCO,
Institut National de Science Appliquées INSA de Strasbourg,
24 Boulvard de la Victoire, 67084 Strasbourg Cedex
France.
E-mail: samia.chiban@insa-strasbourg.fr

ABSTRACT

This work presents a simple model that accurately predicts the deposition from low-concentrated particle-laden turbulent jets in different scenarios. Our proposed model is a developed Lagrangian model that takes advantage of the preferential concentration phenomenon. The unidirectional coupling (fluid-sediment) is used in the modelling. This choice is adopted because when the concentration of solid particles is small enough, it does not affect the hydrodynamic development of the jet. The deposition criterion states that the particle deposits when its settling velocity is greater than the vertical component of the entrainment velocity. Six experiments chosen from the available literature are used to validate the model. These experiments cover the cases of horizontal and inclined buoyant jets in stationary ambient, horizontal buoyant jets in coflow current and nonbuoyant horizontal jets in stationary ambient. Good agreement between the experiments and the obtained simulations is revealed. A sensitivity analysis study is conducted in order to investigate the role of the model main variables. We found that the most important variables are respectively the settling velocity of solid particles, the jet initial velocity, ambient velocity and the buoyancy forces.

NOMENCLATURE

B	[m⁴/s³]	Buoyancy flux;
b	[m]	Jet half-width;
c_f	[-]	Constant in the deposition model;
D	[m]	Port diameter;
E	[kg/s]	Total entrainment;
$f_L(x)$	[m-1]	Longitudinal Particle Density Function (PDF) ordinate;
g	[m/s²]	Gravity acceleration;
g_0	[m/s²]	Reduced gravity $g_0'=g.\Delta\rho/\rho$;
h	[m]	Slice thickness;
ℓ_M	[m]	Jet-plume transition length scale $\ell_M = M_0^{3/4} / B_0^{1/2}$;
M	[m⁴/s³]	Momentum flux;
m	[kg]	Mass in the slice;
P	[kg/s]	Solid flux;
PDF	[-]	Particle Density Function
Q	[m³/s]	Flow (volume flux);
r	[gr/m.s]	Deposition rate;
t	[s]	Time;
u,w	[m/s]	Components of velocity vector;
u_a	[m/s]	Depth-averaged ambient flow velocity;
V	[m/s+ °]	Velocity vector (scalar value +orientation);
v_e	[m/s]	Entrainment velocity;
w_s	[m/s]	Stokes particle settling velocity;
$xb1,xb2,zb1,zb2$	[m]	Cartesian coordinates of the boundaries of the upper surface of the slice;
x,z	[m]	Cartesian coordinates of the centre of the upper surface of the slice;
$zsea$	[m]	Water height above discharge point;
α	[-]	Aspiration entrainment coefficient;
ρ	[kg/m³]	Density;
ϕ	[°]	Jet angle with respect to horizontal plane;
Δm	[kg]	Increase in slice mass due to entrainment; and
ΔS	[m]	Distance along the jet axis from the nozzle to the studied slice.

Subscripts

0	Values at jet discharge point;
a	Ambient values;
j	Values at the end of jet-like region; and
k	Values of slice k " values at k^{th} step of calculation".

INTRODUCTION

The effective or standard submarine outfalls are viable options for the majority of coastal cities for the disposal of partly treated municipal wastewater or treated industrial wastewater, storm water and combined sewer overflows, cooling water and brine effluents from the desalination plants into coastal waters and estuaries.

The suspended solids and hydrophobic pollutants driven to the sea by wastewater impose a real pollution source in the marine milieu that is recently of great interest [1-4]. The suspended solids driven with wastewater deposit near the submarine outfall and alter the water quality and the quality of sedimentation in the seabed.

In the available literature, the study of suspended solids deposition from low concentrated particles-laden jets has been performed for only few scenarios in non-stratified ambient. These studies include experimental studies followed by dimensional analysis [5-7], or followed by Lagrangian modelling [8] or by CFD modelling [9].

As working on low-concentrated jets, all the previous mentioned researches consider that the concentration of solid particles is small enough in the discharge so the presence of these solid particles has no significant influence upon the jet trajectories over a wide range of forcing conditions. Other common considerations for deposition in the near field are considering the solid particles noncohesive, and monodisperse having the same size and shape and thus having one terminal fall velocity w_s which is the velocity value for the ambient fluid density [5,6,8,9]. Finally, all the above experiments and simulations consider the upper surface of the receiving ambient is free and the seabed is considered a flat and horizontal solid boundary.

In practice, the good design of submarine outfall insures that laden solid particles do not deposit in areas adjacent to the discharge point. This condition comes in order to avoid high-polluted seabed areas near the outfall and to avoid the partial or total blockage of the diffuser part. In the same time, the jet initial momentum should not be too high because severe erosion can occur in this case in addition to the considerable structural and economical cost related to affording high momentum jets. The goal of this work is to model sedimentation in the nearfield region. We begin by modelling the development of the nearfield region then modelling the deposition of solid particles. The model is validated and the sensitivity analysis is conducted. Finally we demonstrate a simple example of employing our model in determining the level of upstream treatment for a specific discharge condition in order to prevent deposition in the nearfield.

Nearfield region and the entrainment hypothesis

In ambient water of average density ρ_a, the high momentum wastewater jet creates a zone of low pressure that aspirates the ambient water. In this way, the jet diameter increases; its density and velocity decrease because of the entrainment of ambient fluid till it reaches the sea surface, where it spreads horizontally creating the surface gravity current. The region before the surface gravity current is called the nearfield. We can distinguish in the nearfield itself between two regions (jet-like region and plume-like region). A useful length scale can help in defining the limit between these two zones, it is ($\ell_M = M_0^{3/4} / B_0^{1/2}$) where the initial volume, momentum and buoyancy fluxes are defined respectively as $Q_0=V_0.\pi D^2/4$; $M_0=Q_0.V_0$; $B_0=g_0'.Q_0$. Where V_0 is the jet initial velocity; D is the port diameter; g_0' is the reduced gravity

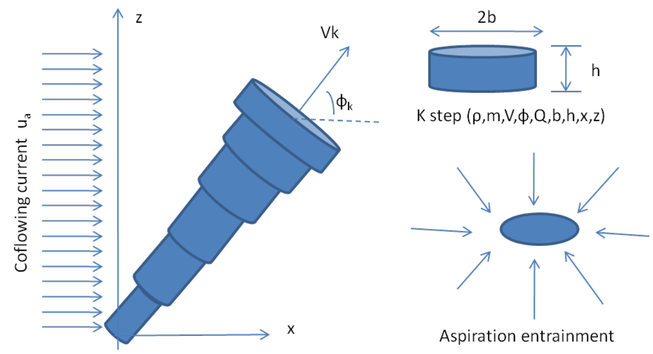

Figure 1 1Lagrangian model for buoyant jet in two-dimensional space.

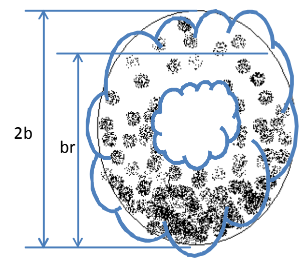

Figure 2 The preferential concentration phenomenon in turbulent jets

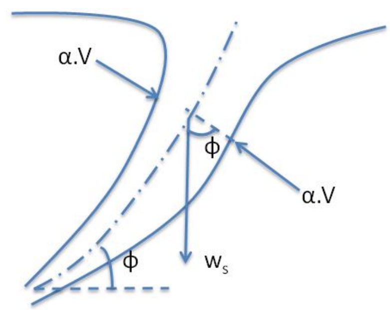

Figure 3 Longitudinal section in the turbulent jet shows the entrainment velocity versus the solid particles settling velocity.

$g_0'=g.(\rho_a-\rho_0)/\ \rho_0$; ρ_0 is the jet initial density; ρ_a the ambient density and g is the gravity acceleration.

In the jet-like region: $\Delta S \le c_j\, \ell_M$ (1)

where $c_j \ge 1$

ΔS is the distance along the jet axis. The value of c_j=1 is adopted in this research following Fischer et al. (1979) [10].

The plume-like region is the region between the jet-like region and the surface gravity current.

In the near field modeling, we present a modified two-dimensional version of the Lagrangian integral model presented by Lee and Cheung (1990) [11]. A cross-sectional slice of the jet is considered with Lagrangian formulation having a coordinate system that moves with the jet as shown in Figure 1. Integration is with time and the calculation takes place at discrete time steps. The slice that is followed is usually the shape of a section of a bent cone as Figure 1 shows. Properties within the slice are assumed to be uniform (top-hat profiles) but vary along the trajectory with time. The size and shape of the slice vary as a result of plume bending, entrainment, and plume growth. The calculation stops when the jet reaches the free surface (in case of buoyant jet) or a prescribed distance (in the case of horizontal non-buoyant jet).

According to the entrainment hypothesis, the equation of mass conservation in stationary ambient can be written

$$\frac{dm}{dt} = E \tag{2}$$

where m is the mass, t is the time, E is the entrainment.

In a Lagrangian framework and a coordinate system that moves with the jet, we can simulate the flow entrained in the jet via the turbulent shear layer. In this work only the aspiration entrainment is considered. This entrainment flux (mass/time) into a slice (k) is the entrainment velocity multiplied by ambient density and slice surface

$$E = Ve_k \cdot \rho_a \cdot 2 \cdot \pi \cdot b_k \cdot h_k \tag{3}$$

The ambient water entrainment velocity Ve is proportional to the centreline velocity via the entrainment coefficient α

$$Ve = |V|_{r=b} = \alpha V \tag{4}$$

Ve is the entrainment velocity, V is the centerline velocity, b is the jet half-width, α is the entrainment coefficient, ρ_a is the ambient density and h is the slice length. In the model presented in this study, we take α as a spatial parameter fitting the acceleration of the jet (α=0.05 to 0.1).

In each time step, we calculate the slice density ρ, mass m, velocity V, inclination ϕ, flow Q, half width b, length h. The slice properties are calculated based on the previous slice properties and on the entrained ambient flow. The loop stops when *zb1(k)<zsea*, where *zb1(k)* is the upper boundary of the jet and *zsea* is the free surface height above the discharge point. In case of non-buoyant horizontal jets, the loop stops when *x(k)<xa*, where *xa* is a prescribed distance from the point source.

The model is explained in the following equations:

The mass in the new slice

$$m_{k+1} = m_k + E_{\alpha_k}.\Delta t \tag{5}$$

The mass difference between two slices

$$\Delta m_k = E_{\alpha_k}.\Delta t \tag{6}$$

The density in the new slice

$$\rho_{k+1} = \frac{m_k.\rho_k + \Delta m_k.\rho_a}{m_{k+1}} \tag{7}$$

The horizontal velocity

$$u_{k+1} = \frac{m_k.u_k + \Delta m_k u_a}{m_{k+1}} \tag{8}$$

The vertical velocity

$$w_{k+1} = \frac{m_k.w_k}{m_{k+1}} + \frac{\rho_a - \rho_{k+1}}{\rho_{k+1}}.g.\Delta t \tag{9}$$

The axial velocity

$$V_{k+1} = \sqrt{u_{k+1}^2 + w_{k+1}^2} \tag{10}$$

The length of the new slice

$$h_{k+1} = V_{k+1}.\Delta t \tag{11}$$

The half-width of the new slice

$$b_{k+1} = \sqrt{\frac{m_{k+1}}{\rho_{k+1}.\pi.h_{k+1}}} \tag{12}$$

The inclination of the jet axis in the new slice,

$$\phi_{k+1} = \arctan\left(\frac{w_{k+1}}{u_{k+1}}\right) \tag{13}$$

The coordinates of the upper surface centre in the new slice

$$x_{k+1} = x_k + u_k.\Delta t \tag{14}$$

$$z_{k+1} = z_k + w_k.\Delta t \tag{15}$$

The coordinates of the boundaries of the upper surface in the new slice

$$\begin{aligned} xb1_{k+1} &= x_{k+1} + b_{k+1}\sin\phi_{k+1} \\ zb1_{k+1} &= z_{k+1} + b_{k+1}\cos\phi_{k+1} \\ xb2_{k+1} &= x_{k+1} - b_{k+1}\sin\phi_{k+1} \\ zb2_{k+1} &= z_{k+1} - b_{k+1}\cos\phi_{k+1} \end{aligned} \tag{16}$$

The distance from the source to the new slice along the jet axis

$$\Delta S_{k+1} = \sum_{k=0}^{k+1} h_k \qquad (17)$$

The ambient fluid entrainment into the new slice

$$E_{\alpha_{k+1}} = \alpha_{k+1}.V_{k+1}.\rho_a.2.\pi.b_{k+1}.h_{k+1} \qquad (18)$$

The first slice (Slice 0) characteristics can be deduced from initial conditions of the jet as follows

$$(u, w)_0 = (V_0 \cos \phi_0, V_0 \sin \phi_0) \qquad (19)$$

The half width b_0 and length h_0

$$(b,h)_0=(0.5D,\ 0.5D) \qquad (20)$$

where D is the nozzle diameter and ϕ_0 is the initial inclination of the jet.

The initial time step, which is taken as a constant in the calculation

$$\Delta t = 0.1 \cdot \frac{h_0}{V_0} \qquad (21)$$

The coordinates of the first slice

$$(x, z)_0 = (0, 0) \qquad (22)$$

For horizontal non-buoyant jets, this routine can be modified where the vertical velocity w is eliminated from all the equations and the calculation stops after a prescribed distance xa. In this case, the Eq. (7) is eliminated because there is no density difference between the two fluids, eq. (9) is eliminated because there is neither initial vertical velocity nor buoyancy forces, and the same for Eqs (13), (15). Based on these eliminations Eqs. (10), (12) (16) and (19) are modified.

PREFERENTIAL CONCENTRATION PHENOMENON

The meaning of the preferential particles concentration in turbulent flow is the formation of concentration inhomogeneity that is related to the fact that the particles, which are more dense than the flow, have the tendency to accumulate in the weak vorticity zones because of the centrifugal force that trains them towards the periphery of the turbulent structures [12].

Based on the preferential concentration phenomenon, we can assume that solid particles deposit from the periphery of the jet. In other words, they deposit from the surface of the ring surrounding the jet core. The deposition takes place from an area of height (br) proportional to the ratio of the jet entrainment velocity to the particle settling velocity as Figure 2 shows.

DEPOSITION CRITERION

We consider that the solid particles deposit when their settling velocity is greater than the vertical component of the entrainment velocity as shown in Figure 3

$$w_s > \alpha_k.V_k.\cos\phi_k \qquad (23)$$

THE PROPOSED MODEL

Our deposition model consists of two formulas: the first formula is for the jet-like region and the second formula is for the plume-like region.

The differential equation of the proposed sedimentation model can be written for the jet-like region as follows

$$\frac{dP}{dS} = -(w_s - \alpha V \cos\phi) C_P.(2b - D). \cdot(1 - \frac{\alpha V \cos\phi}{w_s}).c_f.\alpha\frac{b^2}{D^2} \qquad (24)$$

where P is the solid flux; S is the distance along the jet axis; C_p is the solid particles concentration proportional to the solid flux P and inversely proportional to the volume flux Q as follows:

$$C_p=P/Q \qquad (25)$$

$2b$ is the jet width that presents the outer diameter of the ring and D is the inner diameter.

$(1 - \alpha V \cos\phi / w_s)$ presents the portion of ring involved in the deposition according to the ratio between the two acting forces αV and w_s. This portion is presented in Figure 2 as br.

$c_f.\alpha \cdot b^2 / D^2$ is a parameter used to calibrate the deposition rate in the jet-like region. Where c_f is a constant that presents the role of buoyancy forces in inhibiting the deposition. c_f takes values between 1 and 2 inversely proportional to (g_0'). This parameter is calibrated manually in the cases of nonbuoyant jet and in the presence of coflow current.

Substituting (25) in (24) and rearranging the equation by putting P in the left side:

$$\frac{1}{P}\frac{dP}{dS} = -(w_s - \alpha V \cos\phi)\frac{(2b - D)}{Q} \cdot .(1 - \frac{\alpha V \cos\phi}{w_s}).c_f.\alpha\frac{b^2}{D^2} \qquad (26)$$

Better numerical accuracy can be achieved by rearranging (26) using $\frac{1}{P}\frac{dP}{dS} = \frac{d \ln P}{dS}$

$$\frac{d\ln P}{dS} = -(w_s - \alpha V\cos\phi)\frac{(2b-D)}{Q}.$$
$$(1-\frac{\alpha V\cos\phi}{w_s}).c_f.\alpha\frac{b^2}{D^2} \quad (27)$$

We discretize (27) in a finite difference step forward framework as follows:

$$\frac{\ln P_{k+1} - \ln P_k}{h_k} = -(w_s - \alpha_k V_k\cos\phi_k)\frac{(2b_k-D)}{Q_k}$$
$$.(1-\frac{\alpha_k V_k\cos\phi_k}{w_s}).c_f.\alpha_k\frac{b_k^2}{D^2} \quad (28)$$

The formula which is coupled with the fluid phase model and put in the calculation routine becomes:

$$\ln P_{k+1} = \ln P_k - (w_s - \alpha_k V_k\cos\phi_k)\frac{(2b_k-D)}{Q_k}.$$
$$\cdot(1-\frac{\alpha_k V_k\cos\phi_k}{w_s}).c_f.\alpha_k\frac{b_k^2}{D^2}.h_k \quad (29)$$

At $\Delta S = \ell_M$ the jet-like region ends and the plume-like region begins. In order to keep the continuity between the two regions, the deposition rate in the first slice of plume-like region must equal its value in the last slice of the jet-like region (r_j) (j refers to the last slice "ring" in the jet-like region).

$$r_j = (w_s - \alpha_j V_j\cos\phi_j)\frac{(2b_j-D)}{Q_j}.$$
$$\cdot(1-\frac{\alpha_j V_j\cos\phi_j}{w_s}).c_f.\alpha_j\frac{b_j^2}{D^2}.h_j \quad (30)$$

The deposition model in the plume-like region

$$\ln P_{k+1} = \ln P_k - (w_s - \alpha_k V_k\cos\phi_k)\frac{2(b_k-b_j)}{Q_k}.$$
$$\cdot(1-\frac{\alpha_k V_k\cos\phi_k}{w_s}).h_k - r_j \quad (31)$$

In the case of horizontal nonbuoyant jet, the deposition criterion is $w_s > \alpha_k.V_k$ and because there is no plume-like region, the Eq. (29) is used for the entire studied domain.

MODEL VALIDATION

Six experiments found in the literature are used to validate our model. The six cases are demonstrated in Table 1. The simulation results are shown in Figure 4. We note a good agreement between the experimental data and the model. Case (*a*) presents a horizontal buoyant jet. Case (*b*) presents the case of a buoyant jet inclined-down. Cases (*c,d*) present buoyant jets in coflow current where we note that the majority of solid particles deposit in the nearfield and this is probably due to the moderate current velocity in comparison with the jet velocity. Case (*e*) presents a buoyant jet slightly inclined up in stationary ambient; we note that the mechanism simulated in our model is not the dominant mechanism here but according to the original reference [8], the early deposition here is probably because of some very fine sediments that were carried back over the source region in the surface gravity current and also because the plume will not be fully turbulent until some distance from the source. Case (*f*) presents the deposition from nonbuoyant horizontal jet, the model here well agrees with the experiment data, except in the last part that is probably because of a possible interaction between the jet and the tank bed. Globally we see that the model is in good agreement with experimental data and the mechanism of deposition in the nearfield is the dominant mechanism in almost all of the studied cases.

SENSITIVITY ANALYSIS

Figure (5) shows the sensibility analysis for our model. We take two typical cases, the first is for jets in stationary ambient "case (*a*)" and the second is for jet in coflow current "case (*c*)". We study the effect of jet initial velocity, settling velocity, current velocity and reduced gravity. We change each variable by ±50%. The effect of jet initial velocity and settling velocity are studied for the two cases in Figure 5 (*1,2,4,5*). We note that the important effect of the initial velocity is observed in the first part of the curve 'in the jet-like region' while the effect of settling velocity is obvious along the curve and we note that the cases (*a* and *c*) are affected similarly by the change of these two variables. Figure 5 (*3*) shows the role of coflow current in inhibiting the deposition. In Figure 5(*6*), we see that the reduced gravity has a minor effect on deposition curve; however, the buoyancy force plays a role in dimensioning the nearfield: when this force is significant, the jet will reach the sea surface faster which means less quantity of the particles will deposit in the near-field and vice-versa.

SIMPLE APPLICATION

We consider that the solid particles in municipal wastewater discharged via the submarine outfall are of diameter (*dp*) inferior to 100μm and of average density of 2500 kg/m^3; as the effluent of preliminary treatment.

The application has two objectives: The first is studying the deposition rate in the near field in order to verify if a deposition from this group of particles will take a place in the near-field, and if any, we determine the minimum level of treatment required to avoid the deposition in the near-field. The second objective is determining a minimum 'critical' jet initial momentum above which no deposition will occur for particles of 50μm.

The input data for our model are the jet initial velocity (V_0), the nozzle diameter (D), the density of wastewater (ρ_0), the density of ambient water (ρ_a), the jet initial inclination (ϕ_0),sea depth *zsea*

Table 1. Input data used to calibrate and validate the proposed model

Case	Data source	V_0 m/s	D mm	ρ_0 kg/m^3	ρ_a kg/m^3	u_a m/s	c_f	ϕ_0°	*zsea* m	w_{s0} m/s
a	(Cuthbertson and Davies 2008)[6]	1.04	11.5	1000	1019.6	0	2	0	0.747	0.0299
b	(Lane-Serff and Moran 2005) [8]	0.72	5	1000.3	1040	0	1	-15	0.25	0.027
c	(Cuthbertson and Davies 2008) [6]	1.076	11.5	1000	1019.6	0.038	1.1	0	0.733	0.0299
d	(Cuthbertson and Davies 2008) [6]	1.095	11.5	1000	1038.4	0.038	1	0	0.748	0.0293
e	(Lane-Serff and Moran 2005) [8]	0.66	5	999.65	1040	0	1	17	0.25	0.028
f	(Bleninger et al. 2002) [5]	0.194	6	998.3	998.3	0	1	0	0.192	0.0042

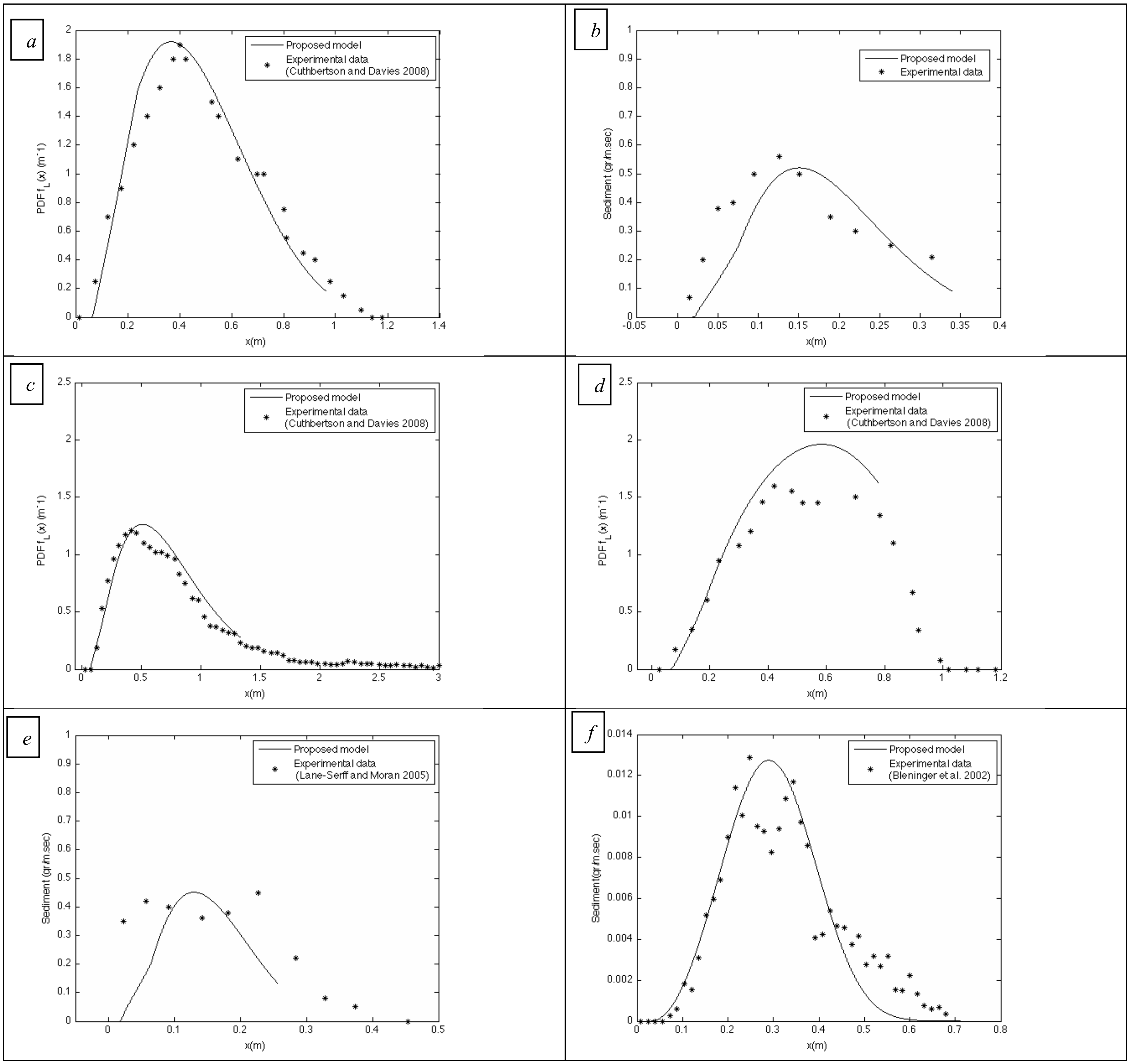

Figure 4 model validation for the cases in Table 1.

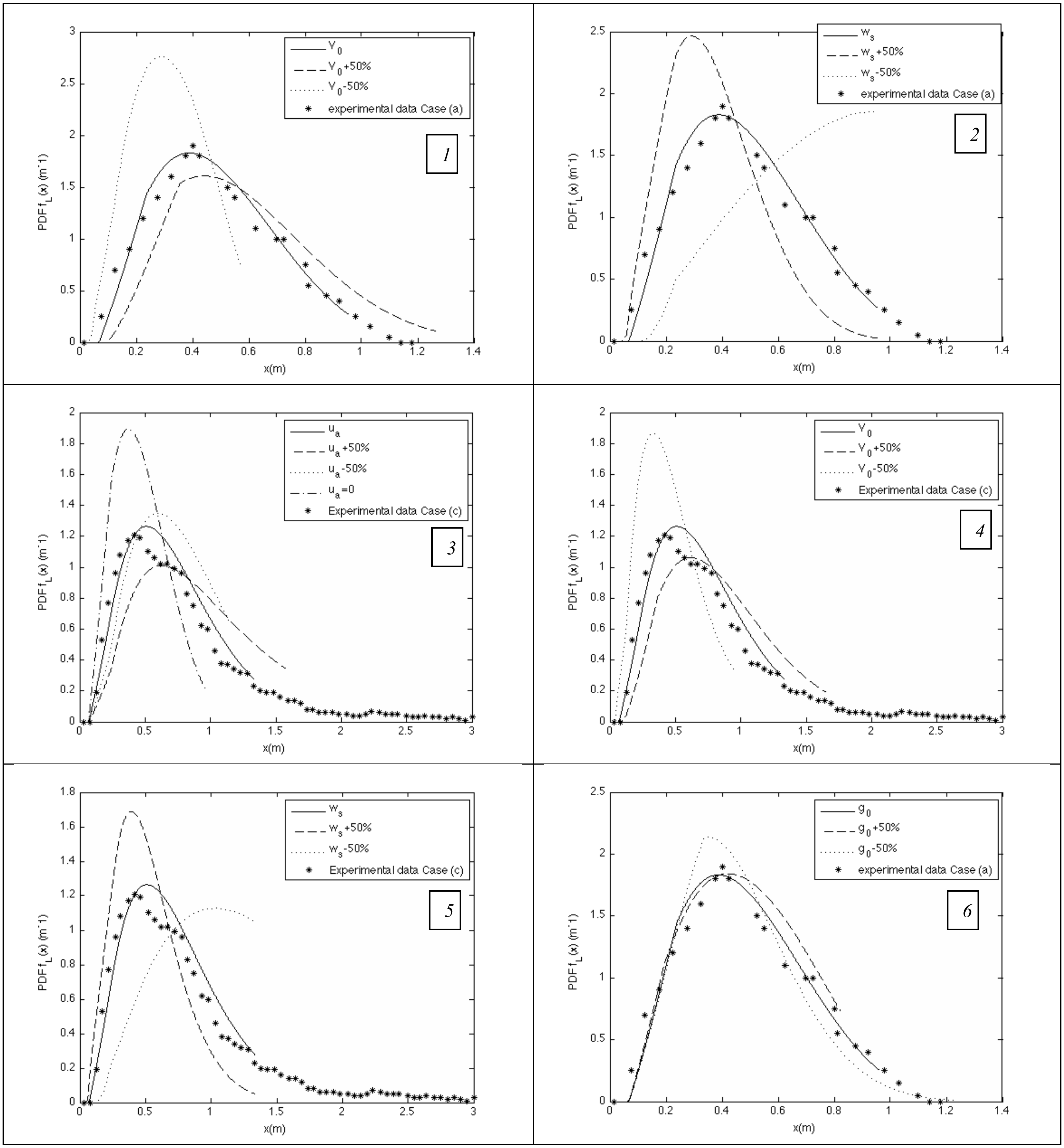

Figure 5 Sensitivity analysis for cases (*a*) and (*c*)

above the discharge point (*zsea*) and the settling velocity of the solid particles (w_s).

As an example we take the following discharge conditions: V_0=4.58 m/s; D=7 cm; ρ_0=1000 kg/m^3; ρ_a =1025 kg/m^3; ϕ_0=15°; zsea=20 m. We find that 94% of particles (*dp*=100 µm) deposit in the near-field while there is no deposition of particles (*dp*=50 µm) in the nearfield. So to avoid deposition in the nearfield we have to adopt an upstream treatment that remove the particles bigger than 50 µm. To know the critical jet initial velocity, we try V_0=3m/s, we find that

8.5% of 50 µm particles deposit in the nearfield, while a V_0=3.5 m/s results in 2.1% of 50 µm particles deposit in the nearfield.

CONCLUSION

Mono-directional coupling between the fluid mouvement and sediment transport was successfuly performed in order to study the deposition from municipal wastewater discharge in natural water. Seven laboratory experiments were selected from literature and used to validate the model. The experiments consist of inclined and horizontal buoyant jets in stationary ambient, horizontal buoyant jet in coflowing ambient and non-buoyant horizontal jet in stationary ambient. In global, the model shows good agreement with experimental data especially when we have high deposition rates from the near-field which makes the deposition mechanism studied here the dominant mechansim. The simulation results are slightly different from the experimental data when other deposition mechanisms are strongly present like deposition from surface gravity current or backward current. Sensitivity analysis is conducted on horizontal jets in stationary ambient and coflow current to study the effect of jet initial velocity, settling velocity, current velocity and reduced gravity. Finally, we take the case of one jet in a multi-port diffuser outfall and we study the fate of discharged particles of diameter 50-100 µm and density 2500 kg/m^3 in order to see which diameter is suspectible to deposit in the near field and thus we will be able to determine the greatest particles diameter that can be discharged in the outfall without depositing in the near-field. A few iterations were sufficient to determine the critical jet initial momentum above which no deposition from particles greater than a certain size is probable in the near-field.

REFERENCES

[1] Chiban, S. Terfous, A. Ghenaim, A. Salman, H. Awad, A., Poulet, J.B. and Sabat M., Sedimentation in the submarine outfall and in the mixing zones (Avoiding, Diagnosis and Remediation), *Journal of shipping and ocean engineering, David publishing*, vol. 1, No. 2, July 2011.

[2] Reopanichkul, P., Carter, R.W., Worachananant S. and Crossland, C.J., Wastewater discharge degrades coastal waters and reef communities in southern Thailand, *Marine Environmental Research*, vol. 69, 2010, pp. 287–296

[3] Sampaio, L. Freitas, R. Máguas, C. Rodrigues A. and Quintino, V., Coastal sediments under the influence of multiple organic enrichment sources: An evaluation using carbon and nitrogen stable isotopes, *Marine Pollution Bulletin*, vol. 60, 2010, pp. 272–282

[4] Lick, W., Sediment and Contaminant Transport in Surface Waters, *IWA Publishing, CRC Press*, 2009, 416 p.

[5] Bleninger, T., Carmer, C., Jirka, G.H. and Neves, M., Sedimentation from low concentration particle-laden jets, *Proc. Int. Conf. Marine Waster Water Discharges* 2002, Istanbul, Turkey, 16.-20.Sep. 2002.

[6] Cuthbertson, A. J. S. and Davies, P. A., Deposition from particle-laden, round, turbulent, horizontal, buoyant jets in stationary and coflowing receiving fluids, *Journal of Hydraulic Engineering,* vol.134, 2008, No. 4, pp. 390-402

[7] Neves, M. J. and Fernando H. J. S., Sedimentation of particles from jets discharged by ocean outfalls: A theoretical and laboratory study" *Journal of Water science and technology,* vol. 32, 1995, No.2 pp 133-139

[8] Lane- Serff, G. F. and Moran T. J., Sedimentation from Buoyant jets, *Journal of Hydraulic Engineering*, vol. 131,2005, No. 3, pp 166-174

[9] Cuthbertson, A. J. S., Apsley, D. D., Davies, P. A., Lipari, G. and Stansby, P. K., "Deposition from particle-laden, plane, turbulent, buoyant jets" *Journal of Hydraulic Engineering*, vol. 134, 2008, No.8, pp. 1110-1122

[10] Fischer, H. B., List, E., J., Koh, R. C.Y., Imberger, J. and Brooks, N. H., Mixing in Inland and Coastal Waters, *Academic Press, New York*. 1979.

[11] Lee, J.H.W. and Cheung, V., Generalized Lagrangian model for buoyant jets in current, *Journal of Environmental Engineering*, vol. 116, 1990, No. 6, pp 1085-1105

[12] Oesterle, B. Ecoulements multiphasiques; des fondements aux méthodes d'ingénierie, *Lavoisier; Paris* 2006.